Anomalous Arctic Sea Ice Melting Linked to Recent Warming Amplification

Juhi Yadav
National Centre for Polar and Ocean Research, Ministry of Earth Sciences (Govt. of India), Goa
Avinash Kumar (avinash@ncpor.res.in)
National Centre for Polar and Ocean Research, Ministry of Earth Sciences (Govt. of India), Goa
Rahul Mohan
National Centre for Polar and Ocean Research, Ministry of Earth Sciences (Govt. of India), Goa
Muthulagu Ravichandran
Ministry of Earth Sciences, Prithvi Bhavan, Lodhi Road, New Delhi 110003

Research Article

Keywords: Tropospheric warming, Arctic amplification, turbulent heat flux, radiative heat flux, and net heat flux

Posted Date: January 11th, 2022

DOI: https://doi.org/10.21203/rs.3.rs-1216059/v1

Abstract

This study investigates the mechanism of seasonal sea ice variation and recent warming amplification. Seasonal temperature changes in the vertical structure reveal that the autumn and winter seasons are warming more than summer. The thermodynamic processes of sea-ice-air interactions via the heat flux component have been studied. The summer Arctic Sea ice has receded by half (~52%), producing excessive heat. This sea ice loss plays a significant role in determining the heat exchange between the ocean and atmosphere in the following season. During a warm season, the ocean heats up due to incident solar radiation. As a result, delayed ice growth and atmospheric warming occur. Sea ice and heat flux feedbacks explain a large part of Arctic atmospheric warming. These abrupt changes are closely coupled to accelerated Arctic Sea ice loss and atmospheric warming, which are still uncertain.

Introduction

Arctic sea ice variability and dynamics are important indicators of climate change [1,2] strongly influenced by ocean-atmosphere forcing [3]. The accelerated decline in Arctic sea ice extent (SIE) was recorded at a rate of -4.7% per decade annually [4]. In contrast, the highest SIE decline was observed in summer ($-76.5\pm6.1 \times 10^3 km^2 yr^{-1}$), and the lowest was observed in spring ($-39.8\pm2.9 \times 10^3 km^2 yr^{-1}$) [5]. Hence, the primary concern of Arctic sea ice studies is seasonal sea ice variability, particularly during summer [6].

Since the satellite era, multiyear ice has decreased dramatically, leading to thinning of Arctic sea ice [7–9]. Changes in sea ice thickness are attributed to the interaction between dynamic and thermodynamic responses [10,11] of sea ice cover to the ocean and atmospheric forcing [12]. In the past four decades, approximately 40% of summer Arctic sea ice has been lost [13], resulting in strong heat transfer from the ocean to the atmosphere through large open seas. Warming in the Arctic has been recorded twice as much as the global temperature average known as Arctic Amplification (AA) [14–17]. According to recent model-based research, the Arctic temperature will rise to 5°C by 2100 [18].

The Arctic ice-albedo process is the primary cause of Arctic sea ice growth and retreat [14]. This process is slowed in the summer because the sea ice begins to melt during the early warming phase, allowing more heat to be absorbed and the sea ice to shrink. In the winter, however, the process is reversed, with cold driving up sea ice growth. Due to variations in the amount of sunlight, ice-albedo feedback mechanisms are weaker in the summer and more robust in the autumn and winter [1,19]. Furthermore, the cold and warm waters from the adjoining seas are driven by wind and accelerate the process of sea ice growth or retreat [20,21]. If current trends continue, the Arctic will have an ice-free summer [22] and be open for trade and commerce soon by the end of this century.

Previous studies have shown that air circulation is a crucial factor in seasonal sea ice variability [8,23]. The atmospheric circulation pattern directly influences Arctic sea ice thermodynamics and oceanic heat flux. Air temperature (AT) has been found to rise across the vertical column of the atmosphere, from the

surface to the high troposphere, resulting in exacerbated Arctic warming [24,25]. There is no clear link between warming in the Arctic and changes in sea ice concentration, sea surface temperature (SST), and Eurasian snow cover [26]. However, direct radiative forcing and poleward heat transfer [27,28] are important factors for upper-tropospheric warming in the Arctic [29].

The decadal trends were computed in this work to determine the dominant spatial pattern of seasonal sea ice and temperature variability in the Arctic region. Furthermore, the thermodynamic processes responsible for seasonal sea ice variability, such as turbulent, radiative, and net heat fluxes, were investigated to comprehend the impact of ongoing seasonal sea ice loss induced by ice-ocean-atmosphere interactions. The primary forces for the rapid melting of sea ice and atmospheric warming aloft the surface have been identified. This study provides new insight into the relative role of thermodynamic forcing in the seasonal variability of Arctic sea ice and vertical variations in atmospheric temperature.

Table 1
The Arctic sea ice extent trends and standard errors from 1979–2020 were calculated. Based on a null hypothesis of zero trends with degrees of freedom 40 (n = 42−2), the R values are highlighted at a significance level of 99% (bold).

	$10^3 km^2 yr^{-1}$	R	$\%Decade^{-1}$
Annual	-56.9±2.5	**-23.03**	-4.7±0.2
Spring	-43.9±3.0	**-14.76**	-3.2±0.2
Summer	-83.2±5.4	**-15.46**	-10.3±0.6
Autumn	-55.0±4.2	**-13.22**	-5.0±0.3
Winter	-46.5±3.1	**-15.19**	-3.0±0.2

Results And Discussion

Since 1979, the total Arctic SIE decadal trend has shown that summer has the highest negative trend (-10.3±0.6% $decade^{-1}$) followed by autumn (-5.0±0.3% $decade^{-1}$), spring (-3.2±0.2% $decade^{-1}$) and winter (-3.0±0.2% $decade^{-1}$) (Table 1). Arctic sea ice declines at a rate of -56.9±2.5 ×$10^3 km^2 yr^{-1}$ throughout the year, with the maximum loss in summer and autumn and the minimum loss in spring. The interannual variation in the Arctic recorded a dipping minimum SIE in 2020 (3.74 million km^2), which is 0.35 million km^2 more than the lowest record of 2012 (3.39 million km^2) [30]. The decadal trend in seasonal Arctic Sea ice and temperature is examined in the following sections to further understand the decadal variation.

Seasonal variations in sea ice and temperature

In the last four decades, the SIC trend in Baffin Bay, the Eastern Greenland Sea, Barents, and the Kara Sea has shown a significant negative trend in all seasons (Fig. 1a-d). Summer experiences, maximum SIE losses throughout the Arctic except for a small region of the central Arctic. The marginal seas have been identified as the area experiencing the most significant loss in decadal SIC from spring to autumn. The SIC and SST have a substantial negative correlation throughout the year, whereas a significant negative correlation (r = −0.95, p <0.01) was observed in summer compared to the other seasons (Table S1). Notably, the Barents Kara region is not permanently frozen, and it has a higher SST (Fig. 1e-h). This is due to the inflow of warmer Atlantic waters, which keeps the area ice-free [11,31,32]. Furthermore, the Arctic is warming rapidly, with temperatures rising by up to 0.5°C at its marginal seas.

There is accelerated heat and energy transfer from the ocean to the atmosphere aided by the lower trend in SIC, and it is primarily linked to the AA [14]. Moreover, the increase in temperature during cold seasons (autumn and winter) is one of the possible reasons for the amplified warming in the Arctic [28]. Similarly, the present study found differential atmospheric warming and cooling in different seasons in the Arctic by analyzing the seasonal and decadal trends of T2M (Fig. 1i-l). We observed a significant positive T2M trend throughout the year, with the highest trend during cold seasons compared to the warm season. During the summer, most of the heat observed from the atmosphere is used to melt the sea ice, resulting in a lower surface temperature (Fig. 1k). On the other hand, the T2M trends in autumn are higher due to the underlying mechanism through which absorbed latent oceanic heat is released back into the atmosphere during the summer. This contrasting behaviour of seasonal T2M is often attributed to the accelerated melting of sea ice, which keeps the surface air temperature near freezing in boreal summer [33,34]. The enhanced heat flow from the exposed open sea surface, rather than ice-albedo feedback, is responsible for amplifying temperature during the cold season [35]. However, the Arctic SIC shows a significant negative correlation with the T2M in all seasons, with the highest correlation in autumn (Table S1). Furthermore, in the following section, we have attempted to determine the mechanism responsible for temperature amplification in the Arctic.

Seasonal Variations in the Vertical Structure of the Atmosphere

The seasonal variations in air temperature (AT) at the vertical level in the Northern Hemisphere (30ºN-90ºN) are shown in Fig. 2. Warm seasons have a lower AT trend than cold seasons, which corresponds to the observations in the previous section. The question is to determine what drives significant warming in the mid- and upper Arctic atmosphere during the cold seasons. The temperature variation of the Arctic atmosphere on the surface and in the air aloft is influenced by the quantity of sea ice cover. As a result, during sea ice melting, surface amplification occurs[14], resulting in stable atmospheric stratification at lower altitudes in the summer. A previous study also found that AT in the Arctic has a highly stable and stratified vertical structure [3].

During the spring season, the negative AT trend is confined to the upper atmosphere (~250 hPa), which suggests that the influence of sea ice loss is constrained to the surface and lower levels of the atmosphere (Fig. 2a) due to limited vertical mixing [27]. The summer AT trend recorded maximum warming in the mid-atmosphere relative to the lower and upper atmospheric AT (Fig. 2b). The positive ice-albedo feedback mechanism is more apparent during the summer. Increased atmospheric heat absorption by the ocean causes the open water to become warmer than the surrounding atmosphere.

In all other seasons, mid-tropospheric warming is most likely due to an imbalance in horizontal energy transmission [28]. The ocean's heat accumulated in the summer was released in the subsequent seasons, as observed in autumn (Fig. 2c). The AT trend in the mid-troposphere of the Arctic during autumn is approximately 0.6°C per decade. The AT trend is positive during the cold seasons due to weak air stratification and greater vertical mixing. The upper troposphere (~250 hPa) warms in the winter due to enhanced vertical mixing of heat and energy from the surface to the atmosphere aloft rather than ice-albedo feedback. Additionally, during the winter, the retreating sea ice and delayed freezing allow for the release of excess heat stored in the ocean [34,36,37]. In the upper troposphere, a negative AT trend (60ºN-90ºN) is recorded in all seasons (Fig. 2a-c) except in winter, which shows a positive AT trend and winter warming (Fig. 2d).

Arctic atmospheric warming above the surface might also be influenced by other possible factors such as cloud cover [38], increased downward LW radiation [35], heat and energy transfer from the lower latitudes, and differential radiative forcing [28]. The following section investigated the role of heat fluxes associated with seasonal variations in Arctic sea ice cover.

Inferring Arctic sea ice changes using THF, RHF, and NHF

This study examined the contribution of ocean-atmospheric heat fluxes to atmospheric warming and stability due to sea ice changes. Interannual and seasonal variations in sea ice cover were also investigated since they increase the interaction between the ocean, ice, and atmosphere.

The seasonal sea ice growth or retreat is driven by the ocean-atmospheric heat exchange process influenced by the THF and RHF. Interannual Arctic sea ice variation is determined primarily by dynamic and thermodynamic mechanisms [39]. The dynamic process involves the movement and accumulation of sea ice to the south, eventually melting. On the other hand, thermodynamics deals with the exchange of heat and energy between the ocean, ice, and atmosphere. Since several other mechanisms function simultaneously, these processes are independent. The earlier study revealed that one-third of the long-term variations in the oceanic heat content in the Arctic result from the fluctuation in ocean-atmosphere heat flux [40]. In response to thermodynamic processes, our study focused on the seasonal change in sea ice.

The surface RHF and THF signs illustrate the direction of ice-ocean-atmosphere interactions. The RHF is governed primarily by the wind speed and AT near the surface, whereas integrals across the entire atmospheric column mainly determine the THF. Reduced sea ice can provide positive surface THF (upward), heat up the atmosphere, and indicate that ice drives the atmosphere. The negative THF (downwards) implies that the atmosphere drives sea ice. The negative NHF is associated with heat from the ocean and vice versa [41]. Accelerated sea ice loss in the Arctic will result in more heat transfer from the ocean to the atmosphere, resulting in atmospheric warming amplification.

A composite analysis was carried out to explain the heat flow process that contributes to atmospheric warming and Arctic Sea ice melting. Arctic Sea ice loss occurs throughout the year, but we considered the heat flux changes only in the negative SIC phase in this study. During the negative SIC phase in spring, the peripheral Arctic seas have negative anomalies, with only the central Arctic experiencing positive anomalies (Fig. 3a). The increasing insolation causes the sea ice to melt with the onset of spring, resulting in a positive THF across the Arctic Ocean, whereas the RHF and NHF are observed to be negative (Fig. 3b-d). A positive LH anomaly has been found in the central Arctic, while a greater negative SH anomaly remains across the Arctic region (Fig. S1). The positive LH and SH fluxes imply that sea ice transfers heat to the atmosphere [42]. Spring SIC had a significant ($p < 0.01$) positive correlation with THF ($r = 0.67$), RHF ($r = 0.52$) and NHF ($r = 0.80$) (Table S1). Furthermore, the positive THF in the Arctic Ocean demonstrates that the ocean surface largely influences the atmosphere, resulting in a higher AT.

Arctic SIC varies most in the summer due to a persistently negative SIC anomaly (Fig. 4a). The summer months demonstrated a similar positive correlation with THF ($r = 0.61$), RHF ($r = 0.86$) and NHF ($r = 0.67$) as the spring months (Table S1). The RHF has the strongest correlation. This could be due to increased incident solar radiation, more open ocean absorbing heat, and considerable reduction in sea ice [15]. In summer, the THF anomaly is weakly positive, while the RHF anomaly is found to be strongly positive in the marginal seas of the Arctic Ocean (Fig. 4b, c). NHF is largely negative during the negative phase of SIC (Fig. 4d). The LH anomaly is negative because most of the heat is absorbed by the ocean (Fig. S2), and it is significantly correlated with the SIC ($r = 0.71$, $p < 0.01$). During summer, the atmosphere loses heat to the ocean, causing increased ocean warming [14]. Hence, atmospheric warming is less than that of the ocean.

In early autumn, a weak positive ice anomaly is observed when the amount of sunlight decreases in the Arctic. However, from the analysis, autumn has the second-highest negative SIE trend (Table 1). The negative phase of SIC in autumn shows maximum sea ice loss in the region surrounding the Central Arctic (Fig. 5a). In contrast to the previous seasons, autumn shows a significant positive and negative correlation with the THF and RHF, respectively (Table S1). The RHF and THF anomalies show positive and negative anomalies, respectively (Fig. 5b, c). Similarly, the NHF does not correlate with the phenomenon that the atmosphere regulates sea ice, but strong positive LW and weak negative SW radiation were observed (Fig. S3). In autumn, the NHF pattern reverses from the previous summer, with positive regions becoming negative (Fig. 5d). The mechanism behind the pattern reversal is probably

related to the fact that heat absorbed in the summer is released in the winter [14,43]. This leads to maximum warming in the autumn and further delays in the subsequent winter when the sea ice freezes.

During the negative winter SIC phase, the composite map shows a weak negative SIC anomaly in the Arctic Ocean with a strong negative anomaly in eastern Greenland and the Barents Kara Sea region (Fig. 6a). The winter SIC primarily depends on the THF and NHF; therefore, increased ocean-atmosphere warming may delay ice formation. The THF anomaly shows a significant positive correlation with SIC (r = 0.35, p <0.1), which is coherent with the findings of spatial distribution (Fig. 6b). However, the RHF anomaly is positive, which is due to dark days (Fig. 6c). There is no correlation between winter SIC and RHF. The NHF anomaly is negative in the Arctic Ocean except in the Barents Kara Sea (Fig. 6d). The variations in the NHF are a cumulative response of the THF and RHF; thus, a decrease in RHF depicts lower NHF. As a result, the SIC and NHF have a lower positive correlation (r = 0.26) than the THF. The correlation analysis revealed significant positive and negative correlations with LH (r = 0.40, p <0.01) and SH (r = -0.26, p <0.10), respectively (Table 1). In winter, the sea-ice-air interaction is largely determined by the LW radiation (Fig. S4).

Summary And Conclusions

Arctic sea ice melting has been a striking feature of abrupt climate change over the past few decades. The Arctic has had a significant negative and positive trend in SIC and temperature (SST and T2M), respectively, with the highest variation in the summer. The long-term annual Arctic SIE record shows a 22% decline since 1979. Summer (52%) is the season with the greatest loss, followed by autumn (27%), spring (15%), and winter (12%). The study shows increased Arctic sea ice loss over the last four decades, linked to an increase in Arctic SST at its periphery. Ocean-ice-atmosphere interactions govern recent Arctic warming during most of the year.

The Arctic atmospheric layer from the surface to the upper troposphere warms year-round. The cold seasons (autumn and winter) record more warming than the warm seasons (spring and summer). The differential atmospheric warming and cooling are due to changes in Arctic sea ice cover, ice-albedo feedback, and the seasonal cycle of ocean-atmosphere heat fluxes. In summer, when the ice-albedo feedback is strong, the upper ocean absorbs heat from the atmosphere. However, the surface layer is cooler in the summer because ice melting and heat transfer consume more energy than heating the atmosphere aloft.

In autumn, the air above the surface is cooler than the ocean surface, allowing energy transfer from the ocean via RHF and THF. Sea ice loss contributes to atmospheric warming, reinforcing heat in the system and delaying ice growth. Winter sea ice loss is lower than summer, but most atmospheric warming is observed in this season. Winter warming causes sea ice to thin and fracture, causing dynamic sea ice movement. It also weakens atmospheric stratification as the Arctic Ocean and nearby continents become warmer due to the thin sea ice cover and open water. As atmospheric stability deteriorates, vertical mixing of the atmosphere and Arctic warming become easier.

During warm seasons, negative albedo increases heat absorption in the ocean, delaying sea ice formation in the following winters and increasing atmospheric warming. Sea ice formation in cold seasons is directly related to the previous season's ocean and atmospheric heating. Melting Arctic Sea ice allows for year-round warming from the surface to the upper atmosphere. Thus, thermodynamic processes are essential to understanding sea ice variation, which drives and responds to Arctic warming. Our findings suggest that Arctic warming is stimulated by seasonal variations in sea ice and ocean-atmosphere heat fluxes. Further work will require a comprehensive analysis to quantify the seasonal contribution to atmospheric warming.

Data And Methods

The study utilized the monthly satellite-derived sea ice extent (SIE) available from the National Snow and Ice Data Center (NSIDC) on a 25 km x 25 km grid from January 1979 to December 2020 in the Northern Hemisphere (www.nsidc.org). These datasets are obtained from ESMR, SMMR, SSMIS and Special Sensor Microwave/Imager (SSM/I), radiance by NASA team algorithms from a Nimbus-7 Scan Multichannel Microwave (SMMR) and Defence Meteorological Satellite Program (DMSP) [9,44].

Monthly averaged reanalysis data of sea ice concentration (SIC), sea surface temperature (SST), air temperature at 2 m (T2M), and vertical levels from 1000 hPa to 200 hPa on 0.25° x 0.25° grid are derived from ERA5 (https://www.ecmwf.int/en/ forecasts/datasets/reanalysis-datasets/era-interim). It is the fifth generation of the European Centre for Medium-Range Weather Forecasts (ECMWF) atmospheric reanalyses of the global climate and weather (https://doi.org/10.24381/cds.f17050d7). The heat flux components taken in the study are based on reanalysis datasets (2.5° x 2.5°) from 1979-2020. The net longwave (LW) radiation, net shortwave (SW) radiation, latent heat (LH) flux, and sensible heat (SH) flux data were obtained from the National Centers for Environmental Prediction/National Center for Atmospheric Research (NCEP/NCAR; https://psl.noaa.gov/data/gridded/data.ncep. reanalysis.html) [45]. All data sets were acquired for the Arctic region (55°N - 90°N) except the vertical air temperature data, which were taken from 30°N - 90°N for the Northern Hemisphere region.

The above monthly averaged datasets were computed for all four seasons - spring (Apr-Jun), summer (Jul-Sep), autumn (Oct-Dec), and winter (Jan-Mar). The net heat flux (NHF) was estimated by numerical-based analysis [46]. The NHF comprises surface turbulent heat flux (LH+SH) and radiation heat flux (LW+SW). The anomalies for all variables are calculated using the differences between the 42-year mean values (1979-2020) and the climatology year (1981-2010). The decadal trend at the seasonal scale for gridded datasets such as SIC, SST, and T2M is based on Student's *t*-test with a significance level of 95%. In addition, a correlation analysis was conducted using two-tailed Pearson's correlation analysis. The correlation coefficients obtained from the analysis are clear indicators of the factors responsible for anomalous sea ice variability.

Additionally, the sensitivity and variability of seasonal ocean-atmosphere heat fluxes have been studied when Arctic Sea ice decreases. The composite analysis was performed based on estimating the

normalized index associated with the interannual variability of the seasonal mean SIC. The global warming signals were removed by detrending the datasets at each grid-point to contemplate the nonlinearities in the analyzed datasets. The years with high/low SIC were chosen based on a normalized index (i.e., the mean subtracted and divided by the standard deviation), exceeding +/−1 values. This method helped make composite maps for RHF, THF, and NHF that demonstrate the prevailing synoptic heat flux conditions associated with the high/low Arctic SIC.

Declarations

Acknowledgements

We gratefully acknowledge the Ministry of Earth Sciences (MoES), New Delhi, for continuous support. Juhi Yadav thanks the University Grants Commission (UGC), New Delhi, India, for the Senior Research Fellowship [No. F.15-6(DEC.2018)/2019(NET)]. The authors sincerely acknowledge various organizations such as the National Snow and Ice Data Center (NSIDC), National Oceanic and Atmospheric Administration (NOAA), Copernicus Marine Environment Monitoring Service, National Centre for Atmospheric Research (NCAR), and European Centre for Medium-Range Weather Forecasts (ERA5) for providing various datasets available in their portals. This is NCPOR contribution no …./2021–22.

Competing interests

The authors declare no Competing Financial or Non-Financial Interests.

Author Contributions

J.Y. and A.K. designed the research. J.Y. performed the numerical experiments and analysis. J.Y. and A.K. performed the analysis and wrote the first draft of the manuscript. J.Y., A.K. and R.M. did the analysis and interpretation of the results. M.R. reviewed the manuscript. All authors contributed and discussed the results for preparing final manuscript draft.

References

1. Serreze, M. C. & Barry, R. G. Processes and impacts of Arctic amplification: A research synthesis. *Glob. Planet. Change* **77**, 85–96 (2011).
2. Yu, L. *et al.* Possible connections of the opposite trends in Arctic and Antarctic sea-ice cover. *Sci. Rep.* **7**, (2017).
3. Deser, C., Walsh, J. E. & Timlin, M. S. *Arctic sea ice variability in the context of recent atmospheric circulation trends*. *Journal of Climate* vol. 13 http://journals.ametsoc.org/jcli/article-pdf/13/3/617/3764151/1520-0442 (2000).

4. Yadav, J., Kumar, A. & Mohan, R. Dramatic decline of Arctic sea ice linked to global warming. *Nat. Hazards* **103**, 2617–2621 (2020).
5. Kumar, A., Yadav, J., Srivastava, R. & Mohan, R. Arctic sea ice variability and trends in the last four decades: role of ocean-atmospheric forcing. in *Understanding Present and Past Arctic Environments* (ed. Khare, N.) 301–324 (Elsevier Inc., 2021).
6. Stroeve, J., Holland, M. M., Meier, W., Scambos, T. & Serreze, M. Arctic sea ice decline: Faster than forecast. *Geophys. Res. Lett.* **34**, (2007).
7. Kwok, R. Arctic sea ice thickness, volume, and multiyear ice coverage: Losses and coupled variability (1958-2018). *Environmental Research Letters* vol. 13 (2018).
8. Maslanik, J., Drobot, S., Fowler, C., Emery, W. & Barry, R. On the Arctic climate paradox and the continuing role of atmospheric circulation in affecting sea ice conditions. *Geophys. Res. Lett.* **34**, L03711 (2007).
9. Cavalieri, D. J. & Parkinson, C. L. Arctic sea ice variability and trends, 1979-2010. *Cryosphere* **6**, 881–889 (2012).
10. Vihma, T., Tisler, P. & Uotila, P. Atmospheric forcing on the drift of Arctic sea ice in 1989–2009. *Geophys. Res. Lett.* **39**, 2501 (2012).
11. Polyakov, I. V., Walsh, J. E. & Kwok, R. Recent changes of Arctic multiyear sea ice coverage and the likely causes. *Bull. Am. Meteorol. Soc.* **93**, 145–151 (2012).
12. Massonnet, F. *et al.* Arctic sea-ice change tied to its mean state through thermodynamic processes. *Nat. Clim. Chang.* **8**, 599–603 (2018).
13. Serreze, M. C. & Stroeve, J. Arctic sea ice trends, variability and implications for seasonal ice forecasting. *Philos. Trans. R. Soc. A Math. Phys. Eng. Sci.* **373**, 20140159 (2015).
14. Screen, J. A. & Simmonds, I. The central role of diminishing sea ice in recent Arctic temperature amplification. *Nature* **464**, 1334–1337 (2010).
15. Cohen, J. *et al.* Recent Arctic amplification and extreme mid-latitude weather. *Nat. Geosci.* **7**, 627–637 (2014).
16. Kumar, A., Yadav, J. & Mohan, R. Global warming leading to alarming recession of the Arctic sea-ice cover: Insights from remote sensing observations and model reanalysis. *Heliyon* **6**, e04355 (2020).
17. Screen, J. A. & Francis, J. A. Contribution of sea-ice loss to Arctic amplification is regulated by Pacific Ocean decadal variability. *Nat. Clim. Chang.* **6**, 856–860 (2016).
18. Tollefson, J. How hot will Earth get by 2100? *Nature* **580**, 443–445 (2020).
19. Cohen, J., Pfeiffer, K. & Francis, J. A. Warm Arctic episodes linked with increased frequency of extreme winter weather in the United States. *Nat. Commun.* **9**, (2018).
20. Overland, J. E. & Wang, M. Large-scale atmospheric circulation changes are associated with the recent loss of Arctic sea ice. *Tellus, Ser. A Dyn. Meteorol. Oceanogr.* **62**, 1–9 (2010).
21. Wu, B., Zhang, R., Wang, B. & D'Arrigo, R. On the association between spring Arctic sea ice concentration and Chinese summer rainfall. *Geophys. Res. Lett.* **36**, L09501 (2009).

22. Boé, J., Hall, A. & Qu, X. September sea-ice cover in the Arctic Ocean projected to vanish by 2100. *Nat. Geosci.* **2**, 341–343 (2009).
23. Ogi, M. & Wallace, J. M. Summer minimum Arctic sea ice extent and the associated summer atmospheric circulation. *Geophys. Res. Lett.* **34**, L12705 (2007).
24. Rigor, I. G., Colony, R. L. & Martin, S. Variations in surface air temperature observations in the Arctic, 1979-97. *Journal of Climate* vol. 13 896–914 (2000).
25. Pithan, F. & Mauritsen, T. Arctic amplification dominated by temperature feedbacks in contemporary climate models. *Nat. Geosci.* **7**, 181–184 (2014).
26. Alexeev, V. A., Esau, I., Polyakov, I. V., Byam, S. J. & Sorokina, S. Vertical structure of recent arctic warming from observed data and reanalysis products. *Clim. Chang.* 2011 *1112* **111**, 215–239 (2011).
27. Screen, J. A., Deser, C. & Simmonds, I. Local and remote controls on observed Arctic warming. *Geophys. Res. Lett.* **39**, 10709 (2012).
28. Graversen, R. G., Mauritsen, T., Tjernström, M., Källén, E. & Svensson, G. Vertical structure of recent Arctic warming. *Nature* **451**, 53–56 (2008).
29. Holland, M. M. & Bitz, C. M. Polar amplification of climate change in coupled models. *Clim. Dyn.* 2003 *213* **21**, 221–232 (2003).
30. NSIDC. Arctic sea ice decline stalls out at second lowest minimum. *Arctic Sea Ice News and Analysis* (2020).
31. Onarheim, I. H., Eldevik, T., Smedsrud, L. H. & Stroeve, J. C. Seasonal and regional manifestation of Arctic sea ice loss. *J. Clim.* **31**, 4917–4932 (2018).
32. Kumar, A., Yadav, J. & Mohan, R. Spatio-temporal change and variability of Barents-Kara sea ice, in the Arctic: Ocean and atmospheric implications. *Sci. Total Environ.* **753**, 142046 (2021).
33. Serreze, M. C., Barrett, A. P. & Cassano, J. J. Circulation and surface controls on the lower tropospheric air temperature field of the Arctic. *J. Geophys. Res. Atmos.* **116**, 7104 (2011).
34. Higgins, M. E. & Cassano, J. J. Impacts of reduced sea ice on winter Arctic atmospheric circulation, precipitation, and temperature. *J. Geophys. Res. Atmos.* **114**, (2009).
35. Kim, K. Y. *et al.* Vertical Feedback Mechanism of Winter Arctic Amplification and Sea Ice Loss. *Sci. Rep.* **9**, 1184 (2019).
36. Deser, C., Tomas, R., Alexander, M. & Lawrence, D. The Seasonal Atmospheric Response to Projected Arctic Sea Ice Loss in the Late Twenty-First Century. *J. Clim.* **23**, 333–351 (2010).
37. Boé, J., Hall, A. & Qu, X. Current GCMs' Unrealistic Negative Feedback in the Arctic. *J. Clim.* **22**, 4682–4695 (2009).
38. Kay, J. E. & Gettelman, A. Cloud influence on and response to seasonal Arctic sea ice loss. *J. Geophys. Res. Atmos.* **114**, 18204 (2009).
39. Kapsch, M.-L., Graversen, R. G. & Tjernström, M. Springtime atmospheric energy transport and the control of Arctic summer sea-ice extent. *Nat. Clim. Chang.* 2013 *38* **3**, 744–748 (2013).

40. Lique, C. & Steele, M. Seasonal to decadal variability of Arctic Ocean heat content: A model-based analysis and implications for autonomous observing systems. *J. Geophys. Res. Ocean.* **118**, 1673–1695 (2013).
41. Kwok, R., Pang, S. S. & Kacimi, S. Sea ice drift in the Southern Ocean: Regional patterns, variability, and trends. *Elementa* **5**, (2017).
42. Cao, Y., Bian, L. & Zhao, J. Impacts of Changes in Sea Ice and Heat Flux on Arctic Warming. *Atmos. Clim. Sci.* **09**, 84–99 (2019).
43. Notz, D. & Marotzke, J. Observations reveal external driver for Arctic sea-ice retreat. *Geophys. Res. Lett.* **39**, (2012).
44. Stroeve, J. & Meier., W. Sea Ice Trends and Climatologies from SMMR and SSM/I, June to September 2001. (2008).
45. Kalnay, E. *et al. 40-Year Reanalysis Project*. *Bull. Am. Met. Soc.* vol. 77 (1996).
46. Budillon, G., Fusco, G. & Spezie, G. A study of surface heat fluxes in the Ross Sea (Antarctica). *Antarct. Sci.* **12**, 243–254 (2000).

Figures

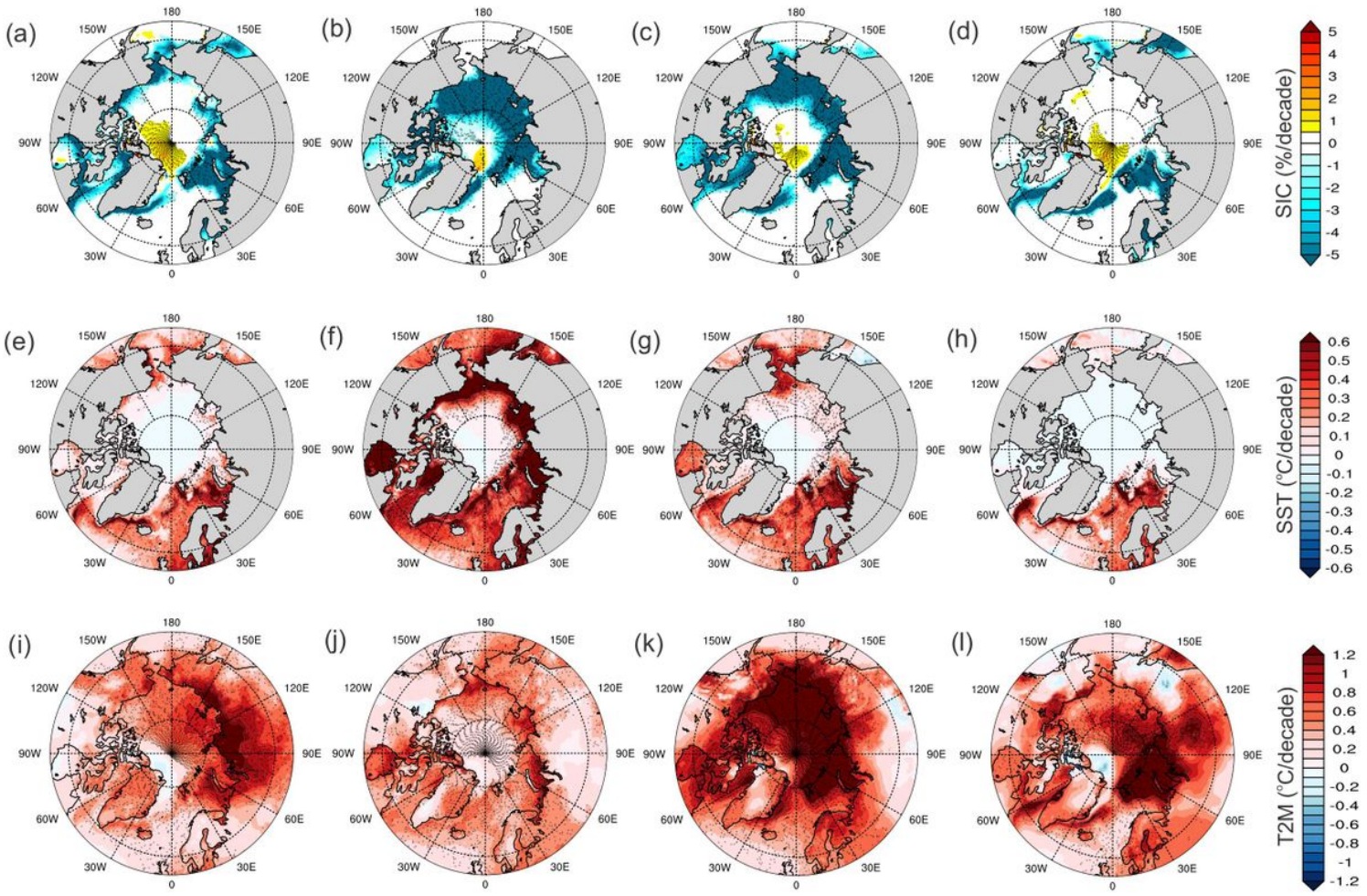

Figure 1

The seasonal Arctic (55°N-90°N) (a-d) SIC (% decade^{-1}), (e-h) SST (°C decade^{-1}), and (i-l) T2M (°C decade^{-1}) trends are shown from 1979 to 2020. The monthly averaged reanalysis dataset was used to estimate the trends. The trends are given for the four seasons: spring (April-June), summer (July September), autumn (October-December), and winter (January-March). The significant trends at the 95% confidence level represented in the black dots are computed using Student's t-test.

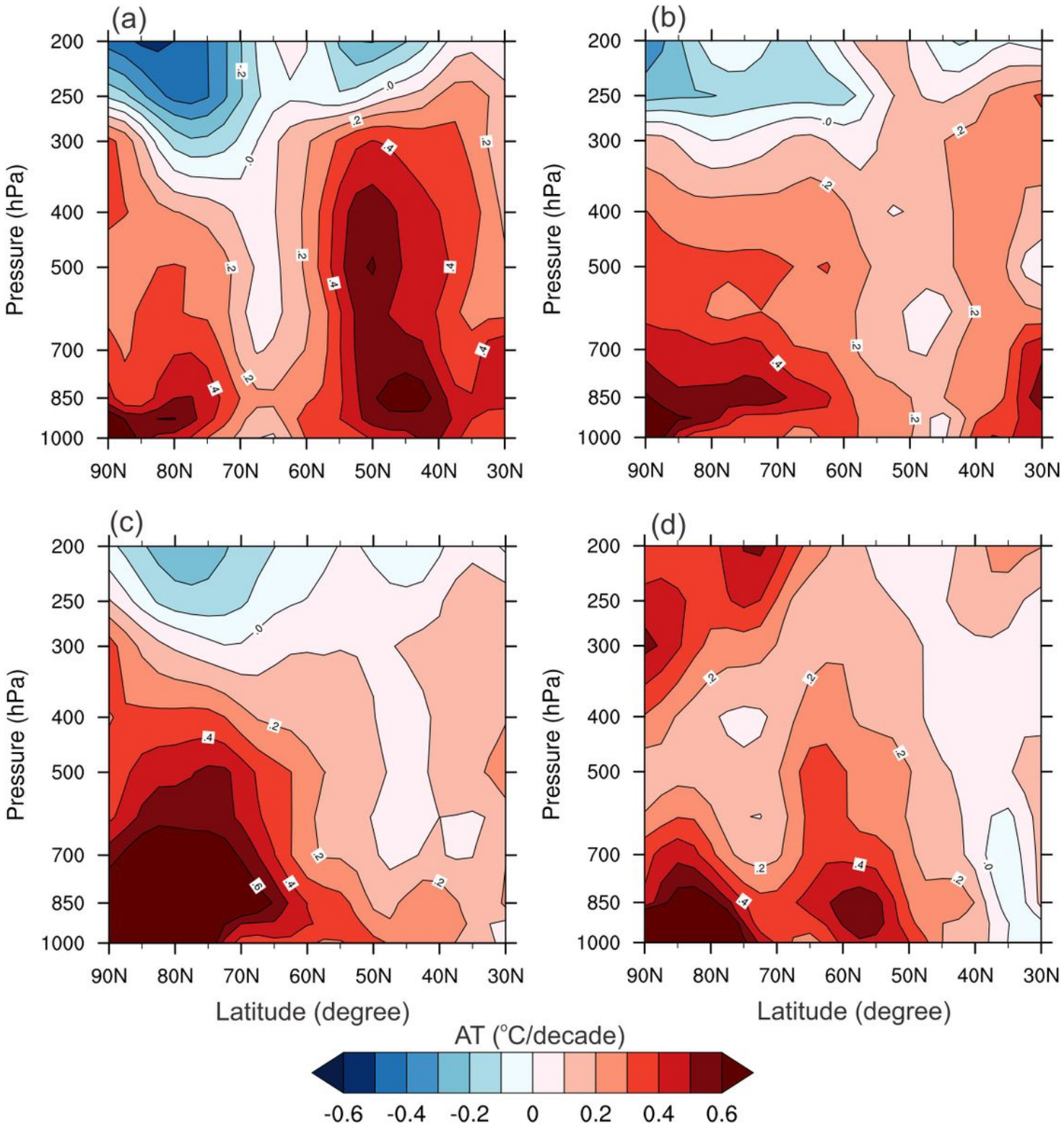

Figure 2

Decadal trends for monthly averaged AT around the circle of the Northern Hemisphere (30°N-90°N) were plotted using latitude versus height (1000-200 hPa). The trends for 1979-2020 are shown for (a) spring, (b) summer, (c) autumn, and (d) winter.

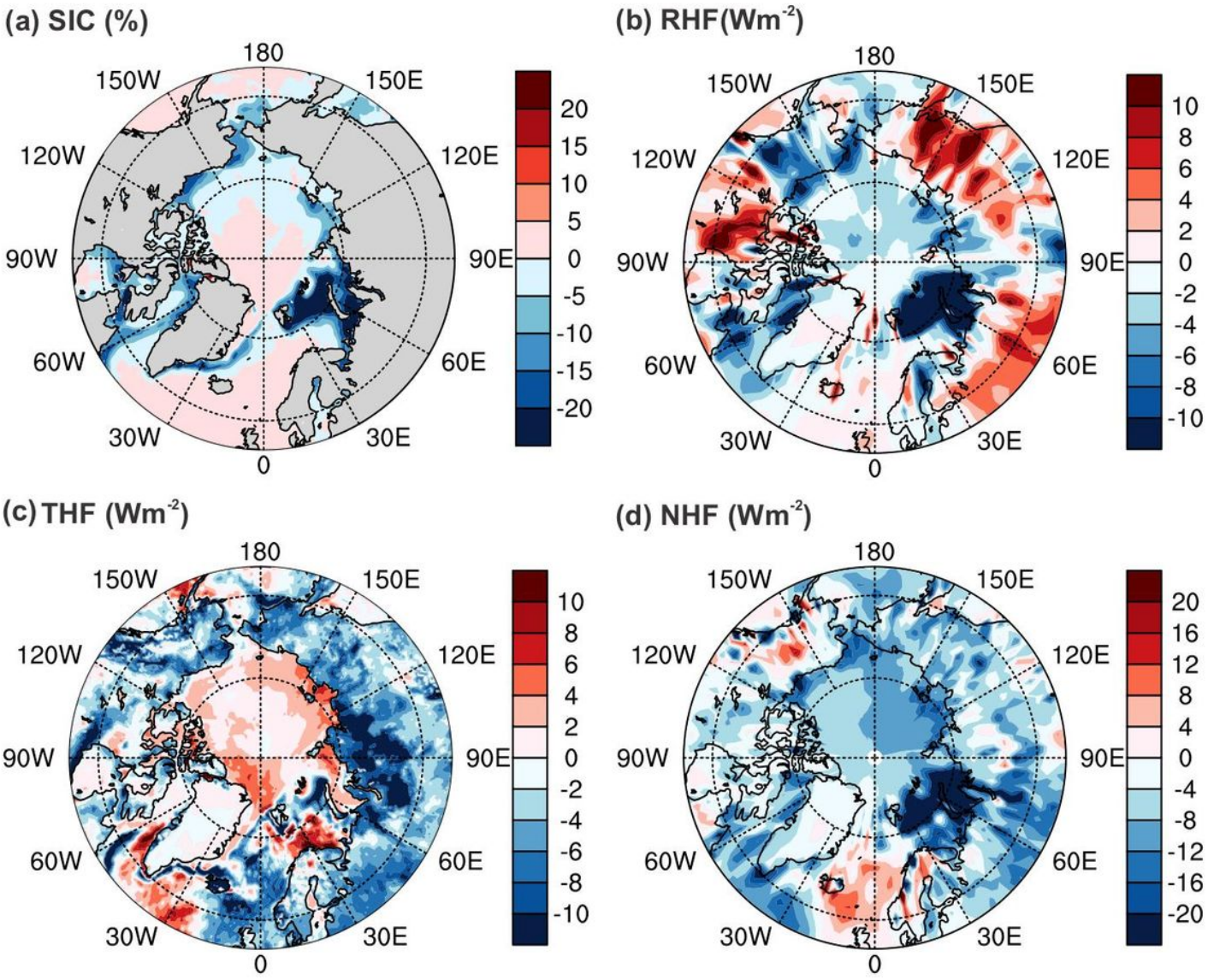

Figure 3

The spatial plot represents a composite anomaly of (a) SIC (%), (b) RHF (Wm^{-2}), (c) THF (Wm^{-2}), and (d) NHF (Wm^{-2}) for the years with low SIC during spring.

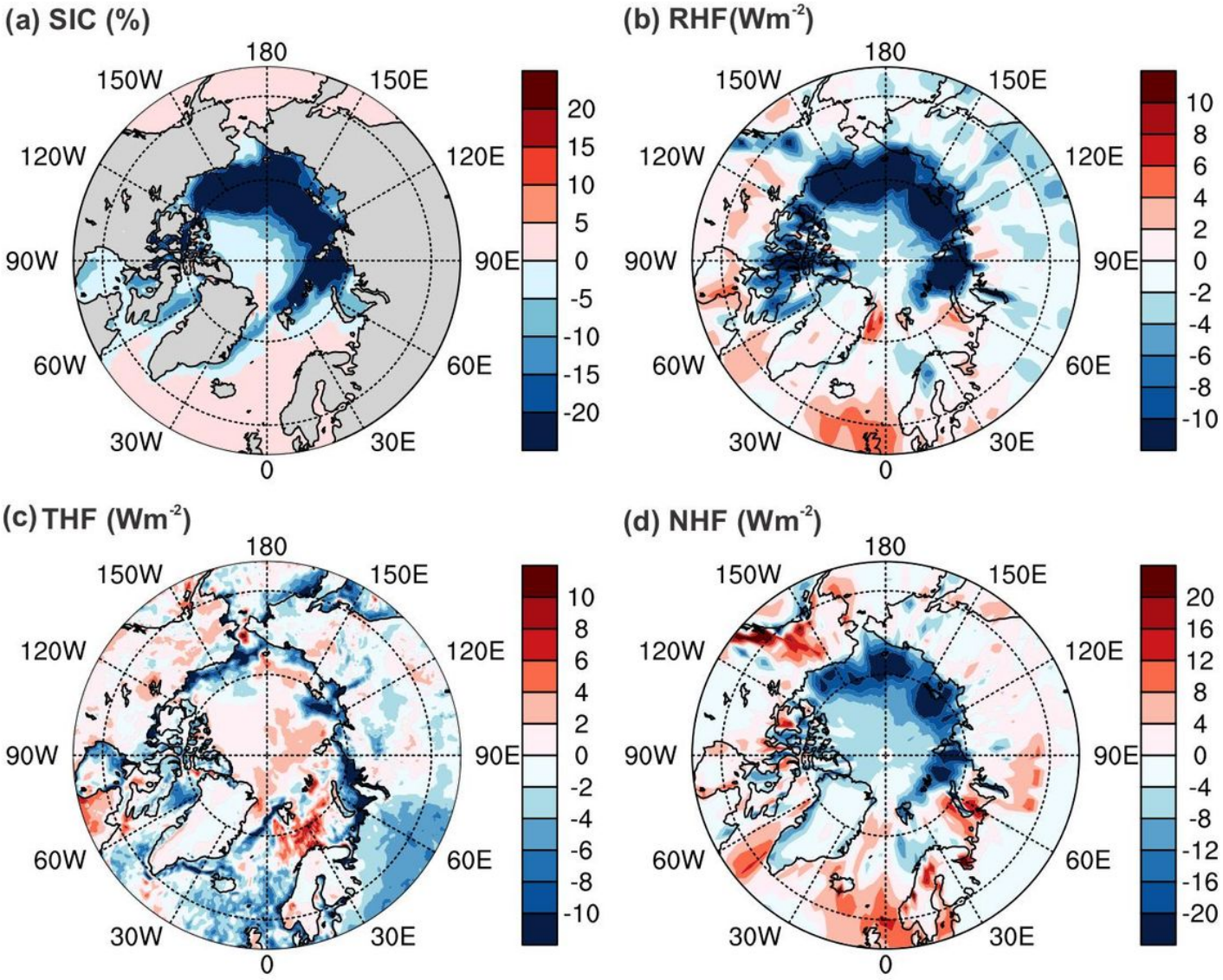

Figure 4

Composite anomaly same as Fig. 3, but for summer.

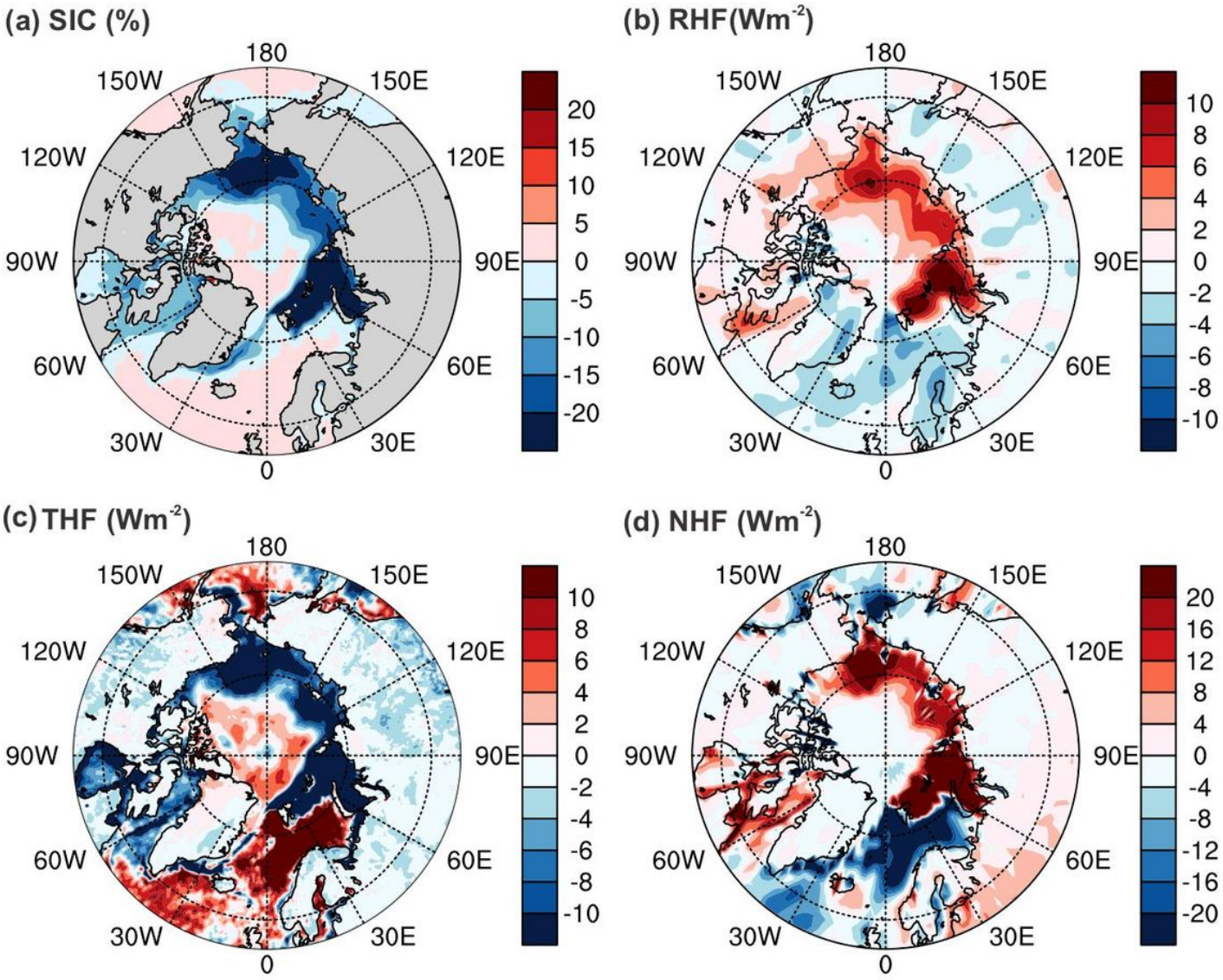

Figure 5

Composite anomaly same as Fig. 3, but for autumn.

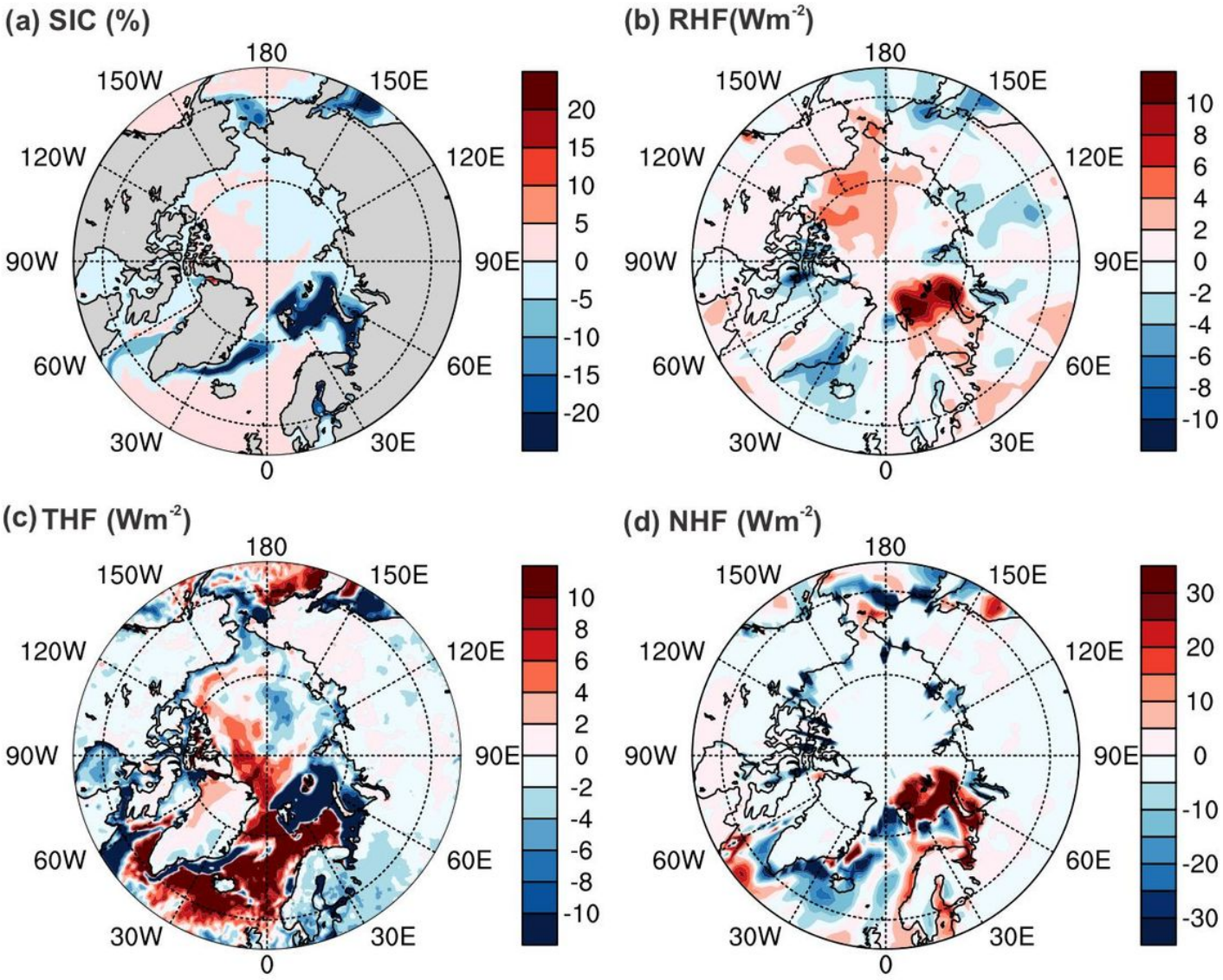

Figure 6

Composite anomaly same as Fig. 3, but for winter.

Supplementary Files

This is a list of supplementary files associated with this preprint. Click to download.

- SupplementaryInformation.docx
- FigureS1.pdf
- FigureS2.pdf
- FigureS3.pdf
- FigureS4.pdf